ACES Asian Chemical Editorial Society

DOI: 10.1002/asia.201800487

CHEMISTRY AN ASIAN JOURNAL Communication

Graphitic Carbon Nitrides

Surface Engineering of Carbon Nitride Electrode by Molecular Cobalt Species and Their Photoelectrochemical Application

Zupeng Chen,[b] Hongqiang Wang,[c] Jingsan Xu,[d] and Jian Liu*[a]

Abstract: Graphitic carbon nitride (CN) has been widely regarded as a promising photocatalyst since the discovery of its capability for photocatalytic hydrogen evolution. Herein, we developed a functional CN film on a conductive fluorine-doped tin oxide (FTO) electrode by using a microprinting-based direct growth method. Furthermore, the photoelectrochemical performance of the derived CN@FTO film was demonstrated to be enhanced by incorporating molecular cobalt species. The reduced charge transport resistance in the cobalt-modified CN@FTO films is suggested to accelerate the charge-carrier transfer rate and thus to improve the performance in photoelectrochemical application. The approach is versatile and can be further optimized by selecting a proper "ink" solution and modifier on various conductive substrates.

The development of light-driven catalysts for water splitting is considered to be an ideal method to convert solar energy.[1] Functional film for photoelectrochemical cell (PEC) exhibits the advantage of efficient charge separation in comparison with the powdered systems.[2] Graphitic carbon nitride (abbreviated as CN) is a promising candidate in diverse applications by taking into account of the low cost and easy access properties, which has been widely utilized as efficient photo-/electrocatalysts for energy conversion, organic transformation, bio-imaging, or used as the supports for other heterogeneous catalysis.[3] However, its utilization towards PEC application is just unfolding and yet to be developed due to the uncontrolled interfacial engineering. The CN film electrode offers a better solution for electron transfer and light harvesting. In this regard, several strategies for fabricating CN films have been developed by different groups (i.e. microcontact printing,[4] sol processing,[5] thermal vapor condensation,[6] electrophoretic deposition[7] and direct growth on substrates[8]). The appropriate precursor selection and the deposition methods determine the film quality and the interfacial engineering.

Cobalt based materials (e.g. Co_3O_4, $Co(OH)_2$, Co-Pi) stand out among numerous water oxidation catalysts due to their earth abundance and low toxicity.[9] The involvement of multiple redox transformation states (Co^{2+}, Co^{3+} and even Co^{4+}) leads to high water oxidation ability.[10] The cobalt species are regarded as the active components for further enhancing the PEC performance of CN based catalysts which relies strongly on the interfacial engineering between cobalt species and photoactive substrates.[11] Based on our experience on the construction of CN film,[4] the molecular Co species are thus intentionally incorporated onto the tri-*s*-triazine framework to enhance the photoelectrochemical performance. The method reported here can be easily extended to any other substrate (e.g., glass, silica wafer, conductive carbons) and the functionality of the CN film can be tailored by applying proper starting "ink" concentrations and doping species.

The cobalt incorporated carbon nitride films on FTO (Co^{2+}-CN@FTO−*x*, *x* = cyanamide concentration) is illustrated in Figure 1. Briefly, an aqueous solution of cyanamide was firstly filtrated into the pore channels within the anodic aluminum oxide (AAO) membranes under vacuum and sonication, which was further sandwiched between two substrates. During the CN thermal condensation, cyanamide acted as the "ink" and was printed and in situ condensed on the substrate in nitrogen atmosphere. Note that the obtained CN films show interconnected archipelagic micro-clusters, inheriting from the periodic channels of the AAO "stamps". The representative scanning electron microscopy (SEM) images of the as-prepared CN films on FTO are illustrated in Figure 2, with films deposited on glass or silicon wafer for comparison (see Figure S1 in Supporting Information). As the PEC properties of the CN films on conductive FTO will be investigated in the following texts, the CN@FTO electrode was carefully studied. A closer look at the SEM images in Figure 2, the derived CN@FTO-60% features a hierarchical morphology. For example, numerous microsized

[a] *Prof. Dr. J. Liu*
College of Materials Science and Engineering
Qingdao University of Science and Technology
Qingdao 266042 (China)
E-mail: liujian@qust.edu.cn

[b] *Dr. Z. Chen*
Department of Colloid Chemistry
Max Planck Institute of Colloids and Interfaces
14424 Potsdam (Germany)

[c] *Prof. Dr. H. Wang*
State Key Laboratory of Solidification Processing, Center for Nano Energy Materials, Shaanxi Joint Laboratory of Graphene, School of Materials Science and Engineering, Northwestern Polytechnical University, Xi'an, 710072 (P. R. China)

[d] *Dr. J. Xu*
School of Chemistry, Physics and Mechanical Engineering, Queensland University of Technology
Brisbane, QLD 4001 (Australia)

Supporting information and the ORCID identification number(s) for the author(s) of this article can be found under: https://doi.org/10.1002/asia.201800487.

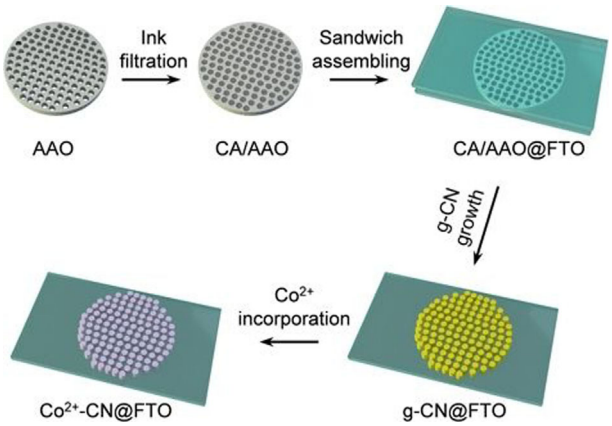

Figure 1. Illustration of the ink printing processes of cobalt-incorporated carbon nitride films on FTO (Co^{2+}-CN@FTO). Abbreviations: AAO, anodic aluminum oxide; CA, cyanamide; FTO, fluorine-doped tin oxide; CN, carbon nitride.

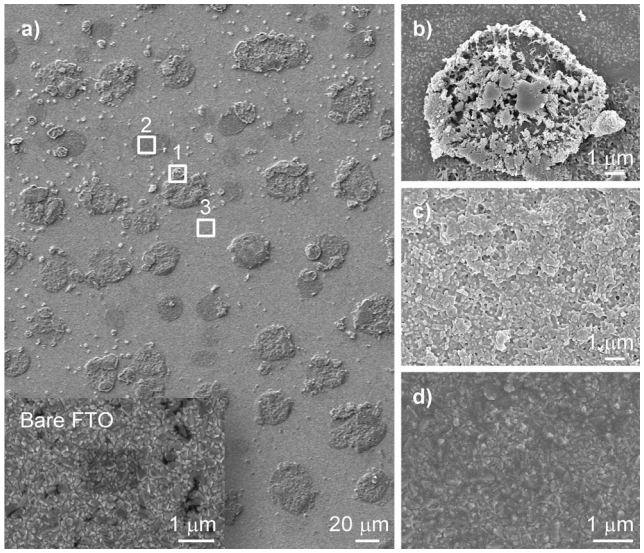

Figure 2. Morphology characterizations of CN films on FTO. a) Large area SEM image of CN@FTO-60%. b–d) Enlarged SEM images of the selected areas in a) marked as 1–3, respectively. The bare FTO substrate was placed in the inset of a) for comparison.

nanowire arrays (region 1) and interweaved bulges with a diameter of 100–200 nm (region 2) are coated on the substrate, which are interconnected by an ultrathin CN layer, as demonstrated by the rough surface of region 3. The corresponding cross-section analysis evidences a continuous ultrathin CN coating (ca. 100 nm thickness) on FTO substrate (Figure S2). The unique hierarchical morphology of the formed carbon nitride films reveals an intricate interplay between the g-CN condensation and decomposition during calcination step. Specifically, the trapped air inside the channels of AAO contributes to the morphology formation by oxidizing the carbon nitride. The confined growth of the CN can be also observed on the surface and within the channels of AAO (Figure S3). In addition, the typical yellow color after calcination hints the formation of CN material.

Fourier transform infrared spectroscopy (FTIR) provides strong evidence for the successful deposition of conjugated aromatic CN heterocycles on the FTO substrates (Figure 3a). Compared with the FTIR spectra of the bare FTO, CN@FTO-60% shows the standard stretching bands between 1200–1600 cm^{-1} assigned to the aromatic C–N and C=N heterocycles, while the breathing mode at 804 cm^{-1} is ascribed to the typical deformation vibrations of the tri-*s*-triazine building unites.[12] Meanwhile, the existence of the terminal NH_x stretching bands above 3000 cm^{-1} and the cyano groups (C≡N) or cumulated double bonds (-N=C=*N*-) at 2200 cm^{-1} indicate the incomplete condensation and presence of surface defect sites.[13] Clear evidence for the formation of CN film from X-ray

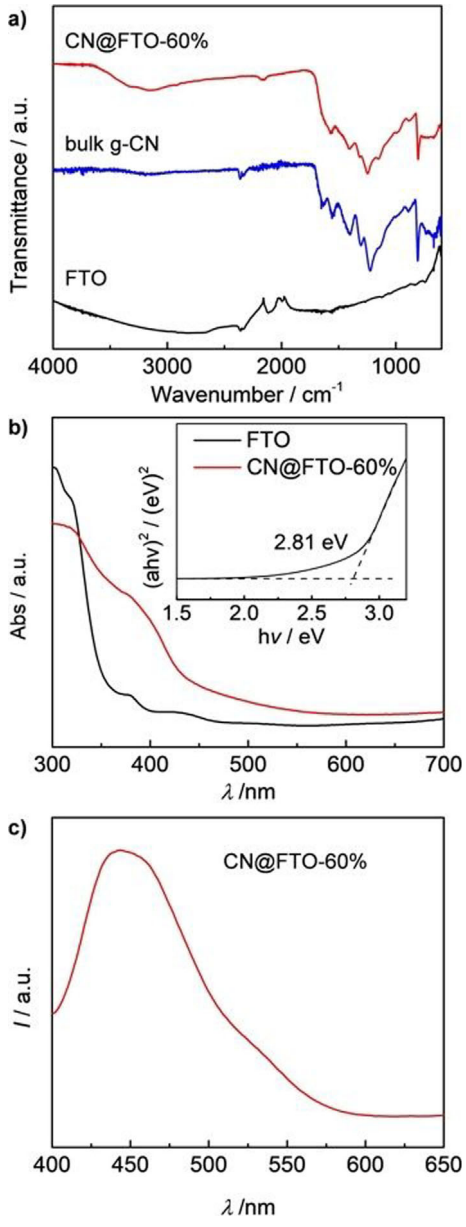

Figure 3. a) FTIR spectra (the bulk g-CN was shown for comparation) b) UV-vis absorption spectra of the CN@FTO-60% film deposited from a 60% cyanamide ink solution and bare FTO subtract (inset shows the corresponding Tauc plots). c) The PL emission spectra of CN@FTO-60% film.

diffraction (XRD) point of view is difficult due to the highly crystalline SnO_2 phase from FTO substrate and the thin film nature. Only a minor peak at 27.3° was observed after subtraction the XRD patterns of FTO from CN@FTO-60% (Figure S**4**), while the bulk CN shows two typical reflections at $2\theta = 13.2°$ (100) and 27.3° (002), stemming from the in-plane repeating units and the graphite-like interlayer stacking layers, respectively. Furthermore, the carbon nitride within AAO channels was assessed after removal of AAO with 2 M HCl, showing similar XRD patterns and FTIR spectra, (Figure S**5**). Meanwhile, the C/N molar ratio of the CN (determined by elemental analysis) from direct condensation of cyanamide and the CN/AAO after HCl etching is 0.69 and 0.71, respectively, which are very close to the theoretical value of 0.75, further confirming the formation of the CN.

The optical properties of the CN@FTO-60% electrode was characterized by UV-vis absorption (Figure 3b) and steady-state photoluminescence (PL, Figure 3c) spectroscopies. Compared to FTO substrate, the absorption spectra of CN@FTO-60% exhibits a typical semiconductor property: the absorption band at $\lambda \approx 450$ nm originates from the π–π^* electron transitions from the highest occupied molecular orbital to the lowest unoccupied molecular orbital.[14] The band gap was calculated to be 2.81 eV (Figure 3b, inset), which is slightly larger than the value for the CN material (2.70 eV) from direct condensation of cyanamide (Figure S6). This hypsochromic shift is presumably caused by the decreased conjugation length within the deposited thin CN films.[15] Moreover, the PL spectra of CN@FTO-60% exhibits a single peak centered at 450 nm, coinciding with its optical absorption spectra (Figure 3c). Similar optical properties can be also observed in the CN film deposited on glass (Figure S**7**).

The successful deposition of tri-*s*-triazine based CN film was further confirmed by X-ray photoelectron spectroscopy (XPS). In general, the C 1s spectra (Figure 4**a**) consist of three contributions at 288.1, 286.4 and 284.8 eV, which correspond to the CN_3 species in the tri-*s*-triazine rings, surface adsorbed hydroxyls and the adventitious carbon contamination, respectively. On the other hand, the N 1s spectra (Figure 4b) can be deconvoluted into three peaks. The main contribution at 398.9 eV is assigned to the ring nitrogen (C-N=C), while the peaks at 400.0 and 400.9 eV are due to the tertiary nitrogen NC_3 and NH_x sites, respectively. Meanwhile, the C–N=C/NC_3 ratio was calculated to be 6, which consists with the tri-*s*-triazine repeating units in CN framework.[16] No signal of cobalt can be observed on the pristine CN@FTO (Figure 4c), while the Co 2*p* spectra of 100 mM $Co(NO_3)_2{\cdot}2H_2O$ treated electrode (100 mM Co^{2+}-CN@FTO) shows two well separated branches of $2p_{1/2}$ and $2p_{3/2}$ at 797.3 and 781.5 eV respectively, which could be ascribed to divalent cobalt.[17] The satellites at around 787.7 and 803.2 eV, are very close to the reported value for Co–N chelating in Co^{II} porphyrin, indicating that the cobalt centers are coordinated to tetradentate N4 ligands.[18] The molecular Co species are expected to be incorporated into the nitrogen rich cavity and the NH_x terminations. The uniform distribution of Co over CN films was confirmed by energy-dispersive X-ray spectroscopy (EDS) mapping (Figure S8).

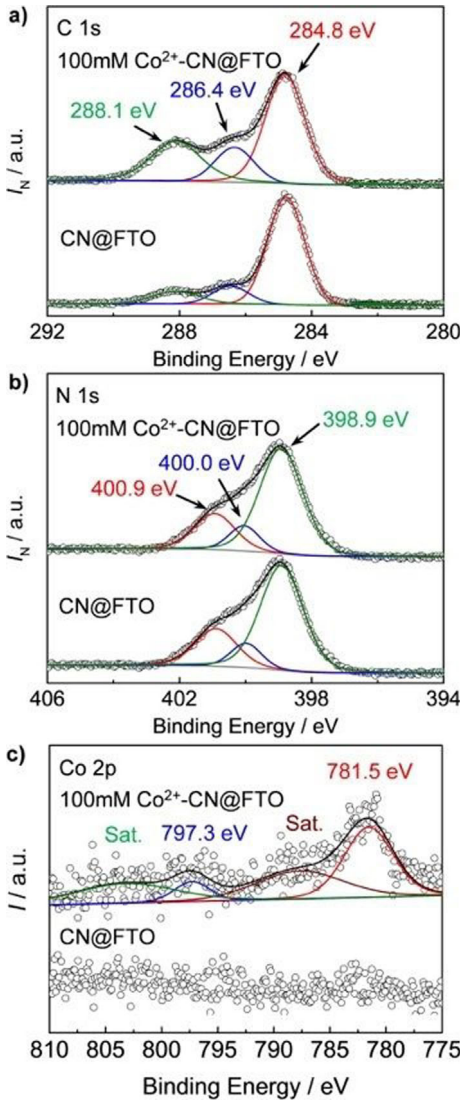

Figure 4. XPS spectra of a) C 1s, b) N 1s and c) Co 2p of 100 mM Co^{2+}-CN@FTO and pristine CN@FTO.

The impact of Co^{2+} incorporation was evaluated in PEC application under illumination and in dark. In order to have a pure correlation between the Co^{2+} concentration and PEC performance, no additive or sacrificial agent was used, and air was removed from electrolyte by purging with nitrogen for 2 h prior to the measurements. As presented in Figure 5a, the onset potential under illumination decreases rapidly from the pristine CN@FTO (1.56 V) to 5 mM Co^{2+}-CN@FTO (1.31 V) and reaches to the optimization on 20 mM Co^{2+} (1.27 V). However, further increasing the Co^{2+} concentration to 50 or 100 mM is detrimental which increases the onset potential back to 1.39 V. In other words, the overpotential was decreased to 1/8 of that for the pristine CN@FTO on 20 mM Co^{2+}-CN@FTO (from 0.32 to 0.04 eV). At the same time, the onset potential for generation of photocurrent is negatively shifted and a smallest value (0.39 V) was achieved at 20 mM Co^{2+}-CN@FTO among all the obtained films (Figure S**9**).

The transient current density at 1.23 V_{RHE} under the chopped light illumination was investigated. It is found that the as pre-

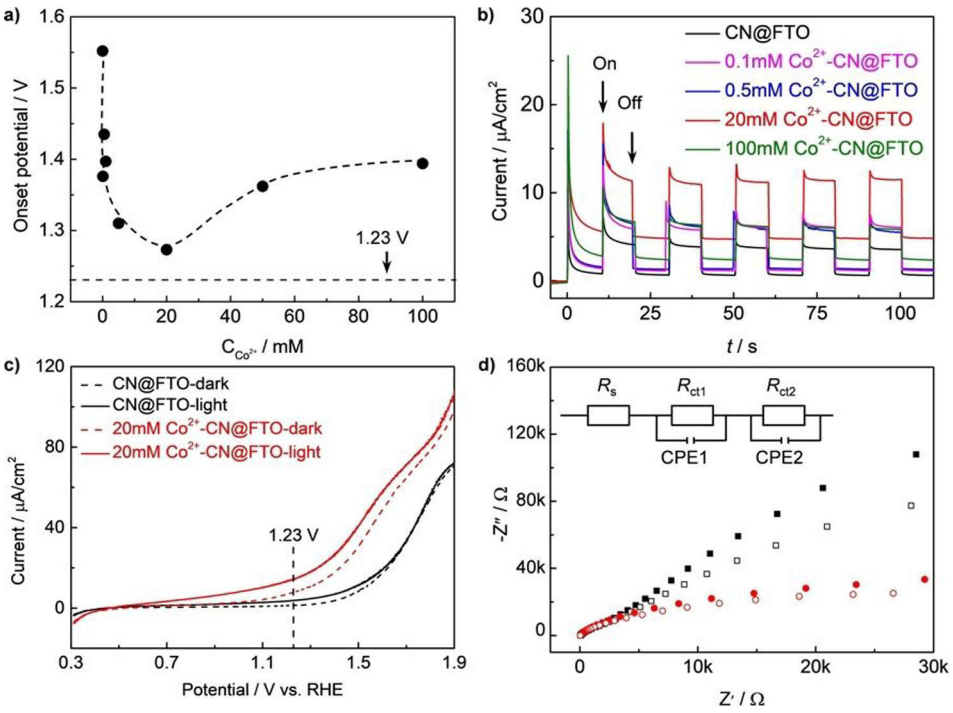

Figure 5. Comparison of a) onset potential under illumination and b) transient current density measured at 1.23 V versus RHE of the CN@FTO-10% electrodes treated with different concentration Co^{2+} (0.1–100 mM); c) LSV curves and d) EIS spectra measured at 1.23 V_{RHE} of CN@FTO-10% and 20 mM Co^{2+}-treated CN@FTO-10% in dark and under illumination. Inset of d) is the equivalent circuit. Symbol codes: black squares, CN@FTO-10%; red circles, 20 mM Co^{2+}-CN@FTO-10%; solid symbols, in the dark; open symbols, under illumination.

pared CN films exhibit a good photo-response property (Figure 5b), generating a transient photocurrent upon switching on and off the illumination. It is obvious that the generated current density shows a rapid decay in the beginning seconds of each on/off cycle, and then reaches a stable current profile. This phenomenon can be explained by the fact that the generated holes are accumulated on the CN film surface, hence these congregated holes recombine with electrons, and consequently resulting in the decay of the photocurrent density.[6a,19] The photocurrent becomes stable once there is balance among the charge generation, separation, transportation and recombination. The highest chopped photocurrent was achieved in the case of 20 mM Co^{2+}-CN@FTO, which is twice as high as that of the pristine CN film (Figure S10). In general, the photocurrent density can be greatly enhanced by employing simulated sunlight and additional sacrificial agents (Na_2SO_3/Na_2S) in basic electrolyte, or marrying with conductive carbon supports such as graphene and carbon nanotubes, which is beyond the scope of current study. Note that the bare FTO showed negligible polarization current either under light or in dark. The CN films behave as n-type semiconductor, as the anodic photocurrents dominate in the present potential window. The linear sweep voltammetry (LSV) curves of 20 mM Co^{2+} treated and the pristine CN@FTO both under illumination and in dark were shown in Figure 5c. It is obvious that the overall current density increases at elevated external bias. Meanwhile, we noticed that the dark current also improves upon increasing the external bias and contributes to the overall current density. Therefore, the net photocurrent at 1.23 V_{RHE} was calculated by subtracting the dark current from the overall current. As can be seen in Figure S11, the net photocurrent reaches peak value for 20 mM Co^{2+}-CN@FTO.

Electrochemical impedance spectroscopy (EIS) was performed at 1.23 V_{RHE} to examine the interfacial charge transport properties along the CN films both under illumination and in dark (Figure 5d). Compared with the pristine CN@FTO, the significant decreased diameter of the semi-cycle in Nyquist plots is observed after 20 mM Co^{2+} modification, thus demonstrating that the charge transport resistance is reduced and therefore the interfacial charge transfer process is accelerated, which on the other hand evidences the carrier mobility effect by Co^{2+} incorporation. The equivalent circuit (Figure 5d, inset) was applied to present the resistance within the system, in which R_s, R_{ct1} and R_{ct2} represent the resistance of the electrolyte, charge transfer resistance at the interface of FTO/film and film/electrolyte, respectively. It is important to mention that the as-prepared CN films are very stable during the PEC measurements and the common problem of peeling off phenomenon was avoided. The pristine morphology of the CN films was retained after PEC measurements (Figure S12).

In summary, a functional carbon nitride thin film was constructed by dispersing molecular Co^{2+} onto microprinted ultrathin carbon nitride on a fluorine-doped tin oxide (FTO) electrode. In comparison to the pristine CN electrode, the 20 mM Co^{2+} treated CN@FTO results in a 2-fold higher photocurrent and significantly reduces the overpotential for water oxidation from 0.32 to 0.04 V, which is ascribed to the reduced charge-transport resistance and accelerated interfacial charge-transfer

process. We believe that the reported versatile approach can be easily extended to fabricate other electronic and photoelectronic devices simply by selecting a proper "ink" and modifier.

Acknowledgements

J. Liu acknowledges the Doctoral Fund of QUST, Thousand Youth Talents Program of China and Natural Science Foundation of Shandong Province (ZR2018MB018). H. Wang acknowledges the financial support from the Fundamental Research Funds for the Central Universities (G2017KY0002), Natural Science Foundation of Shanxi Province (2017JM5028), the National Natural Science Foundation of China (No. 51672225), and Thousand Youth Talents Program of China.

Conflict of interest

The authors declare no conflict of interest.

Keywords: cobalt · electrodes · graphitic carbon nitrides · photoelectrochemical application · thin films

[1] a) K. J. Young, B. J. Brennan, R. Tagore, G. W. Brudvig, *Acc. Chem. Res.* **2015**, *48*, 567 – 574; b) W.-J. Ong, L.-L. Tan, Y. H. Ng, S.-T. Yong, S.-P. Chai, *Chem. Rev.* **2016**, *116*, 7159 – 7329; c) E. S. Andreiadis, M. Chavarot-Kerlidou, M. Fontecave, V. Artero, *Photochem. Photobiol.* **2011**, *87*, 946 – 964.

[2] a) M. Grätzel, *Nature* **2001**, *414*, 338 – 344; b) R. D. L. Smith, M. S. Prévot, R. D. Fagan, Z. Zhang, P. A. Sedach, M. K. J. Siu, S. Trudel, C. P. Berlinguette, *Science* **2013**, *340*, 60 – 63; c) J. Xu, M. Antonietti, M. Shalom, *Chem. Asian J.* **2016**, *11*, 2499 – 2512.

[3] a) Y. Wang, X. Wang, M. Antonietti, *Angew. Chem. Int. Ed.* **2012**, *51*, 68 – 89; *Angew. Chem.* **2012**, *124*, 70 – 92; b) J. Liu, H. Wang, M. Antonietti, *Chem. Soc. Rev.* **2016**, *45*, 2308 – 2326; c) X. Wang, K. Maeda, A. Thomas, K. Takanabe, G. Xin, J. M. Carlsson, K. Domen, M. Antonietti, *Nat. Mater.* **2009**, *8*, 76 – 80; d) J. N. Tiwari, Y.-K. Seo, T. Yoon, W. G. Lee, W. J. Cho, M. Yousuf, A. M. Harzandi, D.-S. Kang, K.-Y. Kim, P.-G. Suh, K. S. Kim, *ACS Nano* **2017**, *11*, 742 – 751; e) X. Zhang, X. Xie, H. Wang, J. Zhang, B. Pan, Y. Xie, *J. Am. Chem. Soc.* **2013**, *135*, 18 – 21; f) Y. Zhao, M. Antonietti, *Angew. Chem. Int. Ed.* **2017**, *56*, 9336 – 9340; *Angew. Chem.* **2017**, *129*, 9464 – 9468; g) Z. Chen, S. Pronkin, T.-P. Fellinger, K. Kailasam, G. Vilé, D. Albani, F. Krumeich, R. Leary, J. Barnard, J. M. Thomas, J. Pérez-Ramírez, M. Antonietti, D. Dontsova, *ACS Nano* **2016**, *10*, 3166 – 3175; h) Z. Chen, S. Mitchell, E. Vorobyeva, R. K. Leary, R. Hauert, T. Furnival, Q. M. Ramasse, J. M. Thomas, P. A. Midgley, D. Dontsova, M. Antonietti, S. Pogodin, N. López, J. Pérez-Ramírez, *Adv. Funct. Mater.* **2017**, *27*, 1605785.

[4] J. Liu, H. Wang, Z. P. Chen, H. Moehwald, S. Fiechter, R. van de Krol, L. Wen, L. Jiang, M. Antonietti, *Adv. Mater.* **2015**, *27*, 712 – 718.

[5] J. Zhang, M. Zhang, L. Lin, X. Wang, *Angew. Chem. Int. Ed.* **2015**, *54*, 6297 – 6301; *Angew. Chem.* **2015**, *127*, 6395 – 6399.

[6] a) J. Bian, Q. Li, C. Huang, J. Li, Y. Guo, M. Zaw, R.-Q. Zhang, *Nano Energy* **2015**, *15*, 353 – 361; b) J. Bian, L. Xi, J. Li, Z. Xiong, C. Huang, K. M. Lange, J. Tang, M. Shalom, R.-Q. Zhang, *Chem. Asian J.* **2017**, *12*, 1005 – 1012.

[7] J. Xu, M. Shalom, *ACS Appl. Mater. Interfaces* **2016**, *8*, 13058 – 13063.

[8] M. Shalom, S. Gimenez, F. Schipper, I. Herraiz-Cardona, J. Bisquert, M. Antonietti, *Angew. Chem. Int. Ed.* **2014**, *53*, 3654 – 3658; *Angew. Chem.* **2014**, *126*, 3728 – 3732.

[9] a) J. Qi, W. Zhang, R. Cao, *Chem. Commun.* **2017**, *53*, 9277 – 9280; b) Y. Wu, L. Wang, M. Chen, Z. Jin, W. Zhang, R. Cao, *ChemSusChem* **2017**, *10*, 4699 – 4703; c) D. Guo, F. Chen, W. Zhang, R. Cao, *Sci. Bull.* **2017**, *62*, 626 – 632.

[10] a) F. Jiao, H. Frei, *Angew. Chem. Int. Ed.* **2009**, *48*, 1841 – 1844; *Angew. Chem.* **2009**, *121*, 1873 – 1876; b) J. Zhang, M. Grzelczak, Y. Hou, K. Maeda, K. Domen, X. Fu, M. Antonietti, X. Wang, *Chem. Sci.* **2012**, *3*, 443 – 446; c) M. W. Kanan, D. G. Nocera, *Science* **2008**, *321*, 1072 – 1075; d) D. K. Zhong, M. Cornuz, K. Sivula, M. Gratzel, D. R. Gamelin, *Energy Environ. Sci.* **2011**, *4*, 1759 – 1764.

[11] a) Y. Zheng, Y. Jiao, Y. Zhu, Q. Cai, A. Vasileff, L. H. Li, Y. Han, Y. Chen, S.-Z. Qiao, *J. Am. Chem. Soc.* **2017**, *139*, 3336 – 3339; b) B. Bayatsarmadi, Y. Zheng, Y. Tang, M. Jaroniec, S.-Z. Qiao, *Small* **2016**, *12*, 3703 – 3711; c) G. Zhang, C. Huang, X. Wang, *Small* **2014**, *11*, 1215 – 1221; d) K. J. McDonald, K.-S. Choi, *Chem. Mater.* **2011**, *23*, 1686 – 1693.

[12] A. Thomas, A. Fischer, F. Goettmann, M. Antonietti, J.-O. Muller, R. Schlogl, J. M. Carlsson, *J. Mater. Chem.* **2008**, *18*, 4893 – 4908.

[13] a) B. V. Lotsch, M. Döblinger, J. Sehnert, L. Seyfarth, J. Senker, O. Oeckler, W. Schnick, *Chem. Eur. J.* **2007**, *13*, 4969 – 4980; b) J. L. Zimmerman, R. Williams, V. N. Khabashesku, J. L. Margrave, *Nano Lett.* **2001**, *1*, 731 – 734.

[14] A. B. Jorge, D. J. Martin, M. T. S. Dhanoa, A. S. Rahman, N. Makwana, J. Tang, A. Sella, F. Corà, S. Firth, J. A. Darr, P. F. McMillan, *J. Phys. Chem. C* **2013**, *117*, 7178 – 7185.

[15] X.-H. Li, J. Zhang, X. Chen, A. Fischer, A. Thomas, M. Antonietti, X. Wang, *Chem. Mater.* **2011**, *23*, 4344 – 4348.

[16] D. Dontsova, S. Pronkin, M. Wehle, Z. Chen, C. Fettkenhauer, G. Clavel, M. Antonietti, *Chem. Mater.* **2015**, *27*, 5170 – 5179.

[17] a) Z. P. Chen, J. Xing, H. B. Jiang, H. G. Yang, *Chem. Eur. J.* **2013**, *19*, 4123 – 4127; b) R. Xu, H. C. Zeng, *Chem. Mater.* **2003**, *15*, 2040 – 2048; c) C. R. Brundle, T. J. Chuang, D. W. Rice, *Surf. Sci.* **1976**, *60*, 286 – 300.

[18] a) T. Lukasczyk, K. Flechtner, L. R. Merte, N. Jux, F. Maier, J. M. Gottfried, H.-P. Steinrück, *J. Phys. Chem. C* **2007**, *111*, 3090 – 3098; b) Y. Jiang, Y. Lu, X. Wang, Y. Bao, W. Chen, L. Niu, *Nanoscale* **2014**, *6*, 15066 – 15072.

[19] X. Lv, M. Cao, W. Shi, M. Wang, Y. Shen, *Carbon* **2017**, *117*, 343 – 350.

Manuscript received: March 30, 2018
Revised manuscript received: April 19, 2018
Version of record online: ■■ ■■, 0000

COMMUNICATION

Graphitic Carbon Nitrides

*Zupeng Chen, Hongqiang Wang, Jingsan Xu, Jian Liu**

■■ – ■■

Surface Engineering of Carbon Nitride Electrode by Molecular Cobalt Species and Their Photoelectrochemical Application

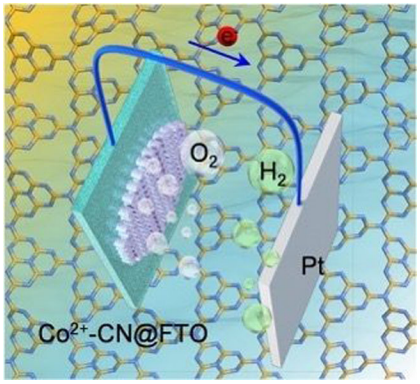

Enhanced photoelectrochemical performance is realized by incorporating molecular cobalt species onto graphitic carbon nitride thin film on a fluorine-doped tin oxide (FTO) electrode, exhibiting the benefits of reduced charge transport resistance and accelerated interfacial charge transfer process, thus significantly depressing the onset potential and overpotential for the water oxidation process.